Article

Folate-Receptor-Mediated Delivery of InP Quantum Dots for Bioimaging Using Confocal and Two-Photon Microscopy

Dhruba J. Bharali, Derrick W. Lucey, Harishankar Jayakumar, Haridas E. Pudavar, and Paras N. Prasad

J. Am. Chem. Soc., **2005**, 127 (32), 11364-11371• DOI: 10.1021/ja051455x • Publication Date (Web): 26 July 2005

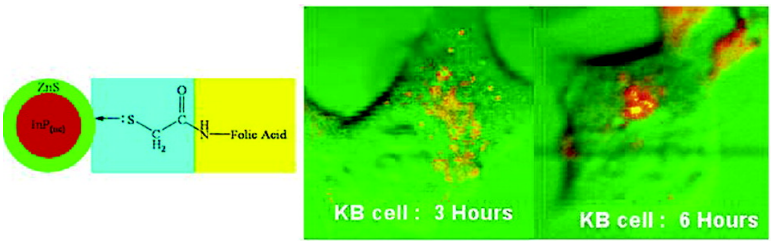

More About This Article

Additional resources and features associated with this article are available within the HTML version:

- Supporting Information
- Links to the 24 articles that cite this article, as of the time of this article download
- Access to high resolution figures
- Links to articles and content related to this article
- Copyright permission to reproduce figures and/or text from this article

View the Full Text HTML

J|A|C|S
ARTICLES
Published on Web 07/26/2005

Folate-Receptor-Mediated Delivery of InP Quantum Dots for Bioimaging Using Confocal and Two-Photon Microscopy

Dhruba J. Bharali, Derrick W. Lucey, Harishankar Jayakumar, Haridas E. Pudavar, and Paras N. Prasad*

Contribution from the Institute for Laser, Photonics and Biophotonics, and Department of Chemistry, The University of Buffalo, The State University of New York, Buffalo, New York 14260-3000

Received March 7, 2005; E-mail: pnprasad@acsu.buffalo.edu

Abstract: A novel method for the synthesis of highly monodispersed hydrophillic InP−ZnS nanocrystals and their use as luminescence probes for live cell imaging is reported. Hydrophobic InP−ZnS nanocrystals are prepared by a new method that yields high-quality, luminescent core−shell nanocrystals within 6−8 h of total reaction time. Then by carefully manipulating the surface of these passivated nanocrystals, aqueous dispersions of folate-conjugated nanocrystals (folate-QDs) with high photostability are prepared. By use of confocal microscopy, we demonstrate the receptor-mediated delivery of folic acid conjugated quantum dots into folate-receptor-positive cell lines such as KB cells. These folate-QDs tend to accumulate in multivescicular bodies of KB cells after 6 h of incubation. Receptor-mediated delivery was confirmed by comparison with the uptake of these particles in folate-receptor-negative cell lines such as A549. Efficient two-photon excitation of these particles and two-photon imaging using these particles are also demonstrated. The use of these InP−ZnS nanoparticles and their efficient two-photon excitation can be potentially useful for deep tissue imaging for future in vivo studies.

Introduction

The use of semiconductor quantum dots (QDs) as luminescence probes for many biological and biomedical applications has become an area of intense research focus over the past few years.[1,2] Particularly, the use of QD as luminescence probes in cell imaging has seen a tremendous amount of effort since the first examples from Alivisatos's and Nie's groups.[3,4] A significant amount of effort has been applied to the synthesis of aqueous dispersions of semiconductor QDs that emit throughout the visible spectra.[3−11] The main attractions for the use of fluorescent QDs as bioimaging probes are their optical and chemical properties such as high photochemical stability, excellent resistance to chemical and photochemical degradation, tunable (size-dependent) photoluminescence (PL) that spans the entire visible spectrum, and good fluorescence quantum yield. Almost all the previous reports of bioimaging with QDs are based on the use of II/VI semiconductor QDs such as CdSe or CdSe−ZnS as luminescence probes. The use of CdTe−CdSe (core−shell) nanocrystals for near-infrared bioimaging has also been reported.[12] CdSe QDs have also found applications in photodynamic therapy.[13]

A widespread replacement of organic fluorophores with II/VI type QDs in bioimaging is hindered by the inherent cytotoxicity of the individual ions (Cd^{2+}, Se^{2-}, and Te^{2-}) that the dots are composed of.[14−17] The quick, short-term solution in general is to grow a thick shell of ZnS on top of the CdSe or CdTe nanoparticles, whose ions are much less toxic. The ZnS shell serves two purposes: (1) it is used for passivating the surface nonradiative recombination sites, thereby improving the quantum yield; and (2) it acts as a barrier whereby CdSe cannot come in contact with the surrounding solvent and thus dissolve through ionization. This is a short-term solution as it allows for successful imaging; however, it does not render the QDs completely safe.[17]

The main advantage offered by III−V semiconductor nanocrystals (as opposed to the II−VI QDs which are already commercially available) lies in the robustness of the covalent bond in III−V semiconductors vs the ionic bond in the II−VI

(1) Prasad, P. N. *Nanophotonics*; Wiley-Interscience: 2004.
(2) Prasad, P. N. *Introduction to Biophotonics*; Wiley-Interscience: 2003.
(3) Bruchez, M.; Moronne, M.; Gin, P.; Weiss, S.; Alivisatos, A. P. *Science* **1998**, *281*, 2013−2016.
(4) Chan, W. C. W.; Nie, S. M. *Science* **1998**, *281*, 2016−2018.
(5) Guo, W. Z.; Li, J. J.; Wang, Y. A.; Peng, X. G. *Chem. Mater.* **2003**, *15*, 3125−3133.
(6) Guo, W. H.; Li, J. J.; Wang, Y. A.; Peng, X. G. *J. Am. Chem. Soc.* **2003**, *125*, 3901−3909.
(7) Gerion, D.; Pinaud, F.; Williams, S. C.; Parak, W. J.; Zanchet, D.; Weiss, S.; Alivisatos, A. P. *J. Phys. Chem. B* **2001**, *105*, 8861−8871.
(8) Parak, W. J.; Gerion, D.; Zanchet, D.; Woerz, A. S.; Pellegrino, T.; Micheel, C.; Williams, S. C.; Seitz, M.; Bruehl, R. E.; Bryant, Z.; Bustamante, C.; Bertozzi, C. R.; Alivisatos, A. P. *Chem. Mater.* **2002**, *14*, 2113−2119.
(9) Jaffar, S.; Nam, K. T.; Khademhosseini, A.; Xing, J.; Langer, R. S.; Belcher, A. M. *Nano Lett.* **2004**, *4*, 1421−1425.
(10) Alivisatos, P. *Nat. Biotechnol.* **2004**, *22*, 47−52.
(11) Gao, X. H.; Cui, Y. Y.; Levenson, R. M.; Chung, L. W. K.; Nie, S. M. *Nat. Biotechnol.* **2004**, *22*, 969−976.
(12) Kim, S.; Lim, Y. T.; Soltesz, E. G.; De Grand, A. M.; Lee, J.; Nakayama, A.; Parker, J. A.; Mihaljevic, T.; Laurence, R. G.; Dor, D. M.; Cohn, L. H.; Bawendi, M. G.; Frangioni, J. V. *Nat. Biotechnol.* **2004**, *22*, 93−97.
(13) Samia, A. C. S.; Chen, X. B.; Burda, C. *J. Am. Chem. Soc.* **2003**, *125*, 15736−15737.
(14) Hoshino, A.; Fujioka, K.; Oku, T.; Suga, M.; Sasaki, Y. F.; Ohta, T.; Yasuhara, M.; Suzuki, K.; Yamamoto, K. *Nano Lett.* **2004**, *4*, 2163−2169.
(15) Chen, F. Q.; Gerion, D. *Nano Lett.* **2004**, *4*, 1827−1832.
(16) Kirchner, C.; Liedl, T.; Kudera, S.; Pellegrino, T.; Javier, A. M.; Gaub, H. E.; Stolzle, S.; Fertig, N.; Parak, W. J. *Nano Lett.* **2005**, *5*, 331−338.
(17) Derfus, A. M.; Chan, W. C. W.; Bhatia, S. N. *Nano Lett.* **2004**, *4*, 11−18.

10.1021/ja051455x CCC: $30.25

semiconductors, which might make them less cytotoxic.[18,19] In fact, Yamazaki et al. have found Syrian golden hamsters given 3 mg/kg InP particles (mean diameter 1.06 μm) intratracheally twice a week for 8 weeks survived throughout a two-year observation period.[20] This makes III−V QDs (e.g., InP) potentially better candidates than II−VI QDs (e.g., CdSe) for biological applications such as bioimaging or photodynamic therapy.[21] So far, InP or other III−V QDs have not been used for bioimaging because they are difficult to prepare on a competitive time scale, and their quantum efficiencies tend to be much lower. Here we report a relatively quick method to produce hydrophobic InP−ZnS core−shell nanoparticles, taking a total of 8 h, with luminescence efficiencies of 10−15%.

Another important aspect in the use of QDs for bioimaging, is the ability to target them to specific organelles or receptors or to certain type of cells, as in the case of organic fluorophores. There are numerous papers discussing targeted delivery of II−VI QDs for imaging of specific cells or cellular organelles.[15,22−27] To demonstrate the targeting capability of these newly synthesized InP/ZnS QDs, we have used folate-receptor targeting. Folate receptors (FR) are one of the many receptors that have been used for drug targeting both in vitro and in vivo. FRs are overexpressed in many of the human cancerous cells, including the malignancies of the ovary, mammary gland, lung, kidney, brain, colon, prostate, nose, and throat; however, they are only minimally distributed in normal tissues.[28] Folic acid, a high-affinity ligand to FR is efficiently internalized into the cell through the receptor mediated endocytosis even when conjugated with a wide variety of molecules.[29−31] Moreover, due to folic acid's high stability, compatibility with both organic and aqueous solvent, low-cost, nonimmunogenic character, ability to conjugate with a wide variety of molecules, and low molecular weight, it has attracted wide attention as a targeting agent.[28,29,32−36]

In this study, we utilize a rapid exchange of encapsulating surfactants with mercaptoacetic acid (MAA), rendering these nanocrystals dispersible in aqueous media and making them available to very easily conjugate with folic acid. We subsequently describe a comparative study of internalization of the QD−folic acid conjugate in KB cells, a human nasopharyngeal epidermal carcinoma cell line overexpressing surface receptor for folic acid as a positive control, and A549 cells, a human lung carcinoma, lacking folic acid receptor as a negative control. Confocal and two-photon imaging, along with localized spectroscopy, were used to confirm the receptor-mediated endocytosis and subsequent internalization of these targeted nanoparticles. To the best of our knowledge, this is the first report utilizing III−V semiconductor QDs as a luminescence probe in bioimaging. Two-photon imaging as well as folic acid targeting of III−V semiconductor QDs is reported for the first time.

Experimental Section

Materials. Zinc acetate and elemental sulfur were purchased from Strem Chemicals. Technical-grade 1-octadecene (90%) was purchased from Aldrich Chemical Co. All solvents were carefully dried by using conventional procedures. All compounds described in this investigation were treated as if they were sensitive to oxygen and moisture and were manipulated either under a purified argon atmosphere in a drybox (Vacuum Atmospheres) or by using standard vacuum line techniques, unless otherwise mentioned. The first chemicals purposefully exposed to air is $InP_{(QDs)}$ upon the completion of their synthesis. Other chemicals such as MAA, folic acid, *N*-hydroxysuccinimide (NHS), dicyclohexylcarbodiimide (DCC), and dimethylsulfoxide having a purity >98% were purchased from Sigma-Aldrich, USA, and used directly without further purification. All the cell lines used in this study were obtained from American Type Culture Collection. All the media used for cell culture were the product of Gibco (USA) cell lines and were purchased from Invitrogen corporation. They were cultured according to instructions supplied from the vendor.

Synthesis of InP−ZnS Nanoparticles. InP QDs ($InP_{(QDs)}$) were prepared by a method originally developed by Lucey et al.[21,37,38] First, the $InP_{(QDs)}$ were prepared as previously described using the following temperatures and conditions. A reaction vessel containing about 1.014 mmol of indium (III) myristate was heated in 40 mL of 1-octadecene (ODE) to 281 °C where approximately 580 μmoles of tris trimethylsilylphosphine ($(TMS)_3P$) was injected rapidly. After 5 s, a reaction equivalent of ODE was added and the reaction temperature was set to 180 °C. After a total of 2 h, the heat source was removed. Upon cooling to room temperature, the reaction mixture was distributed equally between two 50-mL centrifuge tubes. These tubes were centrifuged for 20 min at 3500 rpm, with the temperature set to 20 °C. The supernatant was decanted into two clean centrifuge tubes. Basic calculations were done to determine the amount of zinc and sulfur precursors necessary to produce about a 0.7-nm shell of ZnS. The calculations were based on 100% reaction of phosphorus precursors to form $InP_{(QDs)}$ that were assumed to be 2.0 nm in diameter. From these simple calculations, 1.60 mmol of zinc acetate and 1.65 mmol of elemental sulfur were added to a new reaction vessel within the glovebox. The reaction vessel was removed from the glovebox and attached to the Schlenk line where all of the supernatant, from one of the centrifuge tubes was added (about 40 mL) using a 20-mL airtight syringe. Then using ODE directly from an open container, the reaction volume was adjusted to 100 mL. Next with stirring, a vacuum was established and the temperature was set to 80 °C. After an hour, the reaction vessel was backfilled with argon and the temperature was set to 140 °C. Once the temperature reached 140 °C, the reaction was

(18) Talapin, D. V.; Gaponik, N.; Borchert, H.; Rogach, A. L.; Haase, M.; Weller, H. *J. Phys. Chem. B* **2002**, *106*, 12659−12663.
(19) Kumar, S. Semiconductor Nanochemistry and Hybrid polymer photovoltaics. Ph.D., Albert Ludwigs-Universitat, Freiburg im Breisgan, 2004.
(20) Yamazaki, K.; Tanaka, A.; Hirata, M.; Omura, M.; Makita, Y.; Inoue, N.; sugio, K.; Sigimachi, K. *J. Occup. Health* **2000**, *42*, 169−178.
(21) Lucey, D. W.; MacRae, D. J.; Furis, M.; Sahoo, Y.; Cartwright, A. N.; Prasad, P. N. *Chem. Mater.* **2005**, accepted for publication.
(22) Dahan, M.; Levi, S.; Luccardini, C.; Rostaing, P.; Riveau, B.; Triller, A. *Science* **2003**, *302*, 442−445.
(23) Jain, R. K.; Stroh, M. *Nat. Biotechnol.* **2004**, *22*, 959−960.
(24) Lidke, D. S.; Nagy, P.; Heintzmann, R.; Arndt-Jovin, D. J.; Post, J. N.; Grecco, H. E.; Jares-Erijman, E. A.; Jovin, T. M. *Nat. Biotechnol.* **2004**, *22*, 198−203.
(25) Wu, X. Y.; Liu, H. J.; Liu, J. Q.; Haley, K. N.; Treadway, J. A.; Larson, J. P.; Ge, N. F.; Peale, F.; Bruchez, M. P. *Nat. Biotechnol.* **2003**, *21*, 452−452.
(26) Wu, X. Y.; Liu, H. J.; Liu, J. Q.; Haley, K. N.; Treadway, J. A.; Larson, J. P.; Ge, N. F.; Peale, F.; Bruchez, M. P. *Nat. Biotechnol.* **2003**, *21*, 41−46.
(27) Jaiswal, J. K.; Mattoussi, H.; Mauro, J. M.; Simon, S. M. *Nat. Biotechnol.* **2003**, *21*, 47−51.
(28) Lu, Y. J.; Low, P. S. *Adv. Drug Del. Rev.* **2002**, *54*, 675−693.
(29) Leamon, C. P.; Low, P. S. *Drug Disc. Today* **2001**, *6*, 44−51.
(30) Lu, Y. J.; Sega, E.; Leamon, C. P.; Low, P. S. *Adv. Drug Del. Rev.* **2004**, *56*, 1161−1176.
(31) Asher, S. A.; Peteu, S. F.; Reese, C. E.; Lin, M. X.; Finegold, D. *Anal. Bioanal. Chem.* **2002**, *373*, 632−638.
(32) Leamon, C. P.; Low, P. S. *J. Drug Targeting* **1994**, *2*, 101−112.
(33) Qu, L. H.; Peng, Z. A.; Peng, X. G. *Nano Lett.* **2001**, *1*, 333−337.
(34) Lu, Y. J.; Low, P. S. *Cancer Immunol. Immunother.* **2002**, *51*, 153−162.
(35) Lu, N.; Chen, X. D.; Molenda, D.; Naber, A.; Fuchs, H.; Talapin, D. V.; Weller, H.; Muller, J.; Lupton, J. M.; Feldmann, J.; Rogach, A. L.; Chi, L. F. *Nano Lett.* **2004**, *4*, 885−888.
(36) Ward, C. M. *Curr. Opin. Mol. Therapeut.* **2000**, *2*, 182−187.
(37) Lucey, D. W.; MacRae, D. J.; Prasad, P. N. Process for Producing Semiconductor Nanocrystal Cores, Core-Shell, Core-Buffer-Shell, and Multiple-Layer Systems in a Non-Coordinating Solvent Utilizing *In Situ* Surfactant Generation. WO 2005/002007, March 19, 2004.
(38) Furis, M.; MacRae, D., J.; Lucey, D. W.; Sahoo, Y.; Cartwright, A. N.; Prasad, P. N. *Mater. Res. Soc. Symp. Proc.* **2003**, *789*, 89−94.

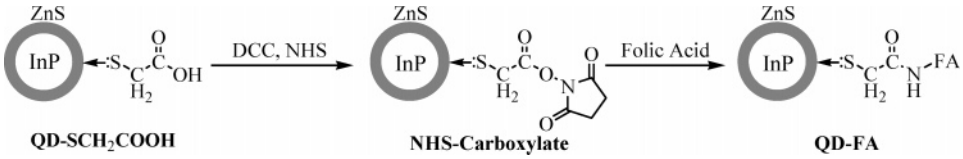

Figure 1. Schematic diagram detailing the preparation of QD−FA.

considered starting. After a total of 1.5 h, the sample was removed from the heat source and allowed to cool to room temperature. Then the entire solution was placed into a one-neck 500-mL round-bottom flask which contained a stir bar. This was connected to the high vacuum line and all volatile materials were removed under vacuum at 60 °C. The flask was left overnight under dynamic vacuum. Then the sample was connected to the Schlenk line where it was backfilled with argon. The entire sample was distributed equally among three centrifuge tubes and centrifuged at 11 000 rpm for 20 min at 20 °C. Then the colorless supernatant was discarded, and the precipitate was combined using a total of about 20 mL of chloroform. After stirring for about 20 min, approximately 15 mL of methyl alcohol and 15 mL of acetone were added and the sample was stirred for an additional 15 min. Again the sample was centrifuged at 11 000 rpm for 10 min at 20 °C. This wash procedure was performed for a total of 3 washes. These nanoparticles were analyzed by optical spectroscopy (UV−vis and PL), dynamic light scattering (DLS) techniques, and X-ray spectroscopy (X-ray diffraction (XRD) and energy-dispersive X-ray spectroscopy (EDXS)).

Preparation of Water-Dispersible InP−ZnS QDs. After isolation of the InP−ZnS core−shell QDs (InP−$ZnS_{(QDs)}$), the surfactant was readily exchanged with MAA. To 15 mg of the dried InP−$ZnS_{(QDs)}$, 10 mL of MAA was added and stirred vigorously for 24 h at room temperature. Then to this solution, 5 mL of chloroform was added and centrifuged at 11 000 rpm for half an hour. The centrifuged pellets were washed with the same amount of chloroform at least three times with repeated centrifugation and dried overnight in an oven at 45 °C. Next, 5 mg of these InP−$ZnS_{(QDs)}$ conjugated with MAA (QD-SCH_2-COOH) were dispersed in 5 mL of PBS buffer (1X), and the excess MAA was removed by dialysis against deionized (DI) water using a 3.5-kD cut off dialysis membrane. Then the whole solution was filtered through a 0.2-μm filter membrane.

Conjugation with Folic Acid. QD SCH_2COOH were conjugated to folic acid by following a standard procedure.[39] To 5 mL of QD SCH_2COOH, 25 μL of DCC (0.05 M solution in DMSO) and an equal amount of NHS (0.05 M solution in DMSO) were added and stirred for half an hour. Finally, 25 μL of folic acid (0.05 M solution in DMSO) was added and stirred overnight. The unreacted materials were separated out by dialysis against DI water for 3−4 h.

The addition of DCC and NHS to the QD SCH_2COOH forms a highly reactive intermediate (NHS−carboxylate), which can react subsequently with the free amino group present in folic acid, as shown in Figure 1, to form the resulting QD SCH_2COOH conjugated with folic acid (QD−FA).

Optical Spectroscopy. UV−vis absorption spectra were recorded in a quartz cuvette with a 1-cm path length using either a Shimadzu UV-3101PC UV−vis−NIR scanning spectrophotometer or a Hewlett-Packard 8452A diode array spectrophotometer. Fluorescence spectra were taken on a Fluorolog-3 spectrofluorometer (Jobin Yvon, Longjumeau, France). For the single-photon emission spectra, the excitation wavelength (λ_{ex}) were 400 nm with slit widths of 1 nm each, and the spectra were recorded from 415 to 785 nm. A Ti:sapphire laser (Tsunami from Spectra-Physics) pumped by a diode-pumped solid-state laser (Millenia, Spectra Physics) was used as a source (~100-fs pulses at 82 MHz) for two-photon excitation. The experimental setup used for obtaining two-photon excitation spectra of QDs is similar to the one previously reported.[40] Excitation cross sections of QDs from 720 to 880 nm were determined using Rhodamine B solution (100 μM solution in methanol) with known two-photon excitation cross section[41] as standards.

Energy Dispersive X-ray Spectroscopy (EDXS). The elemental composition and the purity of the InP−ZnS QDs were determined by using a Hitachi S-4000 field emission scanning electron microscope. The microscope operates at an electron acceleration voltage of 20 kV. The sample is cast as a thin film from the dispersion or simply used as a powder on a silicon or graphite substrate. The X-ray fluorescence beams are collected with an X-ray collection unit IXRF 500 system.

Transmission Electron Microscopy (TEM). The size and the morphology of the folic acid conjugated QDs were examined by using a JEOL JEM-100CX transmission electron microscope. One drop of this QD−FA was mounted on a thin film of amorphous carbon deposited on a copper grid (300 mesh).

Dynamic Light Scattering (DLS). The effective size and size distribution of the QD suspensions were estimated by Brookhaven Instruments Corp. of Holtsville, NY utilizing their dynamic light scattering particle size analyzer (Brookhaven 90Plus fitted with APD detector using a 656-nm laser). InP QDs and InP−ZnS were dispersed in hexanes with 0.1 volume % octylamine at a concentration of 1 mg/mL. QD−FA particles were dispersed in 1× PBS at the same concentration. These solutions were repeatedly filtered through a 0.1-μm syrringe filter membrane to remove the dust impurities and then analyzed directly.

Cell Culture. Human nasopharyngeal epidermal carcinoma cell line (KB) and a human lung carcinoma cell line (A549) were respectively maintained in minimum essential medium (MEM) with 10% FBS and F12K media with 10% FBS, according to the manufacturers instructions (American Type Culture Collection). To study the uptake and imaging of the conjugated folic acid, the cells were trypsinized and resuspended in the corresponding suitable media at a concentration of around 7.5×10^5 mL^{-1}. Then, 60 μL of this suspension was transferred to each 35-mm culture plate, and 2 mL of the corresponding full medium was added. These plates were then placed in an incubator at 37 °C with 5% CO_2 (VWR Scientific, model 2400). After 36 h of incubation, the cells (50% confluency) were rinsed with PBS, and 2 mL of the corresponding fresh media was added to the plates. Finally, 100 μL of QD−FA was added and mixed properly. Plates were returned to the incubator (37 °C, 5% CO_2) for the required incubation period. After each specific time interval of incubation (1, 2, 3, 6, and 18 h), the plates were taken out and rinsed several times with sterile PBS, and 2 mL of fresh serum free medium was added. The plates were incubated for another 10 min at 37 °C and were directly imaged under a confocal microscope. To confirm the receptor-mediated uptake, competition experiments were conducted where the cell culture was pretreated for 1 h with 50 μL of 1 mM folic acid solution prior to QD−FA treatment.

Confocal Microscopy. Confocal as well as two-photon imaging were performed using a confocal laser scanning microscope (MRC-1024, Bio-Rad, Richmond, CA), which was attached to an upright microscope (Nikon model Eclipse E800). A water immersion objective lens (Nikon, Fluor-60X, NA 1.0) was used for cell imaging. The Ti:sapphire laser was tuned to a center wavelength of 800 nm (~100-fs pulses at 82

(39) Hermanson, G. T., *Bio Conjuagate Techniques*; Academic Press: New York, 1996.

(40) Chung, S. J.; Maciel, G. S.; Pudavar, H. E.; Lin, T. C.; He, G. S.; Swiatkiewicz, J.; Prasad, P. N.; Lee, D. W.; Jin, J. I. *J. Phys. Chem. A* **2002**, *106*, 7512−7520.

(41) Xu, C.; Webb, W. W. *J. Opt. Soc. Am. B* **1996**, *13*, 481−491.

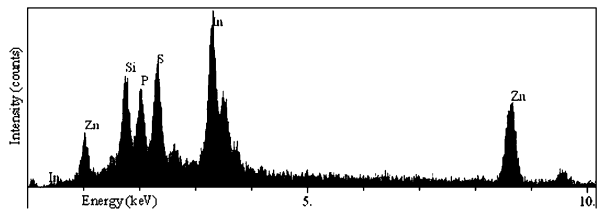

Figure 2. EDXS spectrum of InP−ZnS nanoparticles.

MHz) to use as the source for two-photon excitation. The laser was coupled into the microscope scan head using beam-steering optics. For single-photon imaging, the same Ti:sapphire output, tuned to 840 nm, was doubled by second harmonic generation (SHG) in a β-barium borate (β-BBO) crystal to obtain the 420-nm light and was coupled into a single mode fiber for delivery into the confocal scan head. A combination of long-pass and short-pass filters were used to cut off the excitation light from entering the detection channels. (Long pass filter OG515 and short pass filter 720SP, both from Chroma technology Corp.) To distinguish autofluorescence from the QD emission, we have also used localized spectrofluorimetry.[42] For this purpose, the fluorescence signal was collected, without filtering, from the upper port of the confocal microscope, using a multimode optical fiber of core diameter 1 mm, and was delivered to a spectrometer (Holospec from Kaiser Optical Systems, Inc.) equipped with a cooled charge-coupled device camera (Princeton Instruments) as a detector.

Result and Discussion

Structural Properties of InP−ZnS QDs. The prepared InP−ZnS core−shell nanoparticles ($InP-ZnS_{(QDs)}$) were characterized by X-ray spectroscopy (XRD and EDXS), electron microscopy (TEM), DLS, and optical spectroscopy (spectrofluorimetry, UV−vis). The purity of the newly prepared $InP-ZnS_{(QDs)}$ was confirmed by the EDXS as shown in Figure 2.

It is evident that the only elements present in the sample are indium, phosphorus, zinc, silicon, and sulfur. The silicon is a result of trace silicon grease used on the reaction flask during the synthesis. Carbon, hydrogen, and oxygen, which make up the surfactant, cannot be detected by this technique and thus are not evident.

The crystallinity of QDs is best determined by XRD of the material. We have found $InP_{(QDs)}$ and InP−ZnS nanocrystals to be highly crystalline, as demonstrated by the XRD spectra in Figure 3.

The bulk lattice parameters of cubic InP and ZnS are displayed in the figure. It is important to note that the diffraction of the core−shell material does not change dramatically, and this is common when the effective mass of the shell material is very small in comparison to the core material.[43−45] By utilization of the Scherer equation, we calculated the diameter of the core $InP_{(QDs)}$ to be 26.1 Å, using only the ⟨111⟩ indices. The diameter of the core−shell InP−ZnS nanoparticles are not calculated because the formation of the ZnS layer causes the ⟨111⟩ reflection to shift to higher 2θ value which also causes a slight broadening of the reflection. Thus the Scherer equation no longer

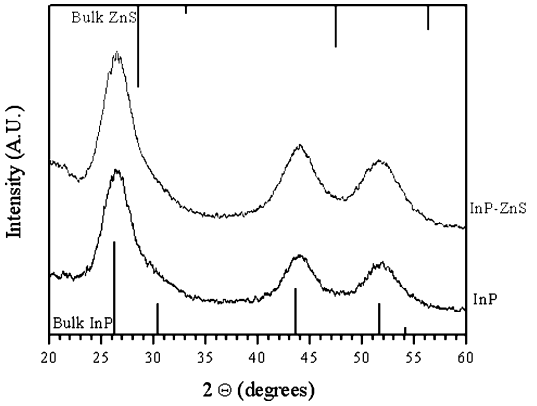

Figure 3. XRD of InP and InP−ZnS nanoparticles.

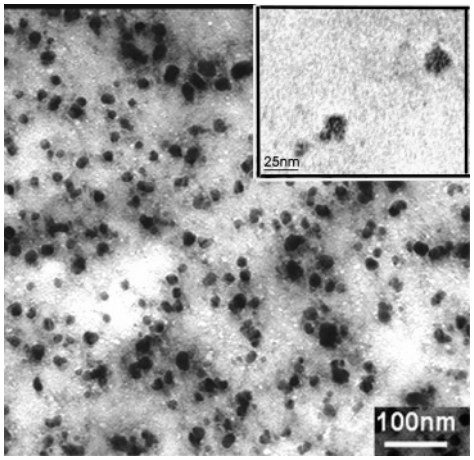

Figure 4. TEM image of QD−FA nanoparticles. Inset shows a higher magnification image of the same particles.

holds when a new material is over coated onto a pure core. On the basis of our approximations and the amount of precursors used, the thickness of the ZnS shell surrounding the InP core is approximately 1 monolayer.

Figure 4 shows the TEM image of folic acid conjugated $InP-ZnS_{(QDs)}$ (QD−FA). From TEM it is clear that the QD−FAs are spherical in shape and have a size of 10−20 nm in diameter. Significant clustering of particles is evident.

DLS has also been used to measure the size distribution of prepared nanoparticle suspensions. Figure 5 contains the effective size as well as size distributions of InP, InP−ZnS suspensions in hexanes, and QD−FA suspended in PBS.

From the plots it is evident that the InP QDs in hexanes have an effective diameter of 4.0−5.7 nm, with the InP−ZnS nanoparticles demonstrating an effective diameter of 4.9−12.6 nm and the QD−FA nanoparticles demonstrating an effective diameter of 15.1−26 nm. On the basis of these data, the initial InP QDs are relatively monodisperse. The InP−ZnS QDs are larger and may have formed clusters of two to three individual QDs to make up the larger, 12.6 nm particles. Within the QD−FA samples there was significant clustering in solution as the 15−26 nm size can only be explained as clusters of mutiple individual InP−ZnS particles. The TEM image agrees well with this result. From the higher magnification image, it is evident that mutiple QDs are visible within each nanocluster.

(42) Wang, X.; Pudavar, H. E.; Kapoor, R.; Krebs, L. J.; Bergey, E. J.; Liebow, C.; Prasad, P. N.; Nagy, A.; Schally, A. V. *J. Biomed. Opt.* **2001**, *6*, 319−325.
(43) Dabbousi, B. O.; RodriguezViejo, J.; Mikulec, F. V.; Heine, J. R.; Mattoussi, H.; Ober, R.; Jensen, K. F.; Bawendi, M. G. *J. Phys. Chem. B* **1997**, *101*, 9463−9475.
(44) Huang, G.-W.; Chen, C.-Y.; Wu, K. C.; Ahmen, M. O.; Chou, P.-T. *J. Cryst. Growth* **2004**, *265*, 250−259.
(45) Peng, X. G.; Schlamp, M. C.; Kadavanich, A. V.; Alivisatos, A. P. *J. Am. Chem. Soc.* **1997**, *119*, 7019−7029.

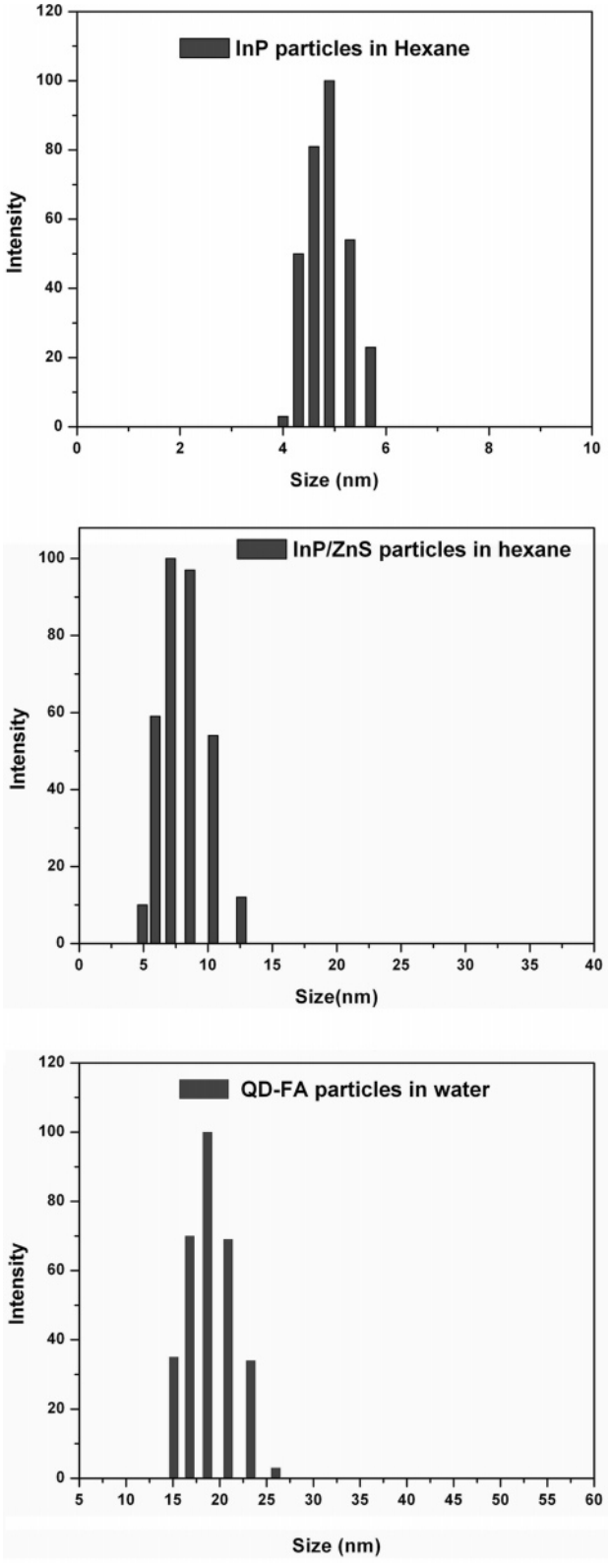

Figure 5. DLS data showing the size distribution of InP and InP/ZnS QDs in hexane and QD−FA in water.

According to our XRD results, the average size of the InP particles is 26.1 Å. This does not directly agree with the DLS data; however, XRD only measures the size of the inorganic semiconductors and does not consider the organic capping ligand. The results of the DLS experiments demonstrate the effective diameter, which includes the size of the organic

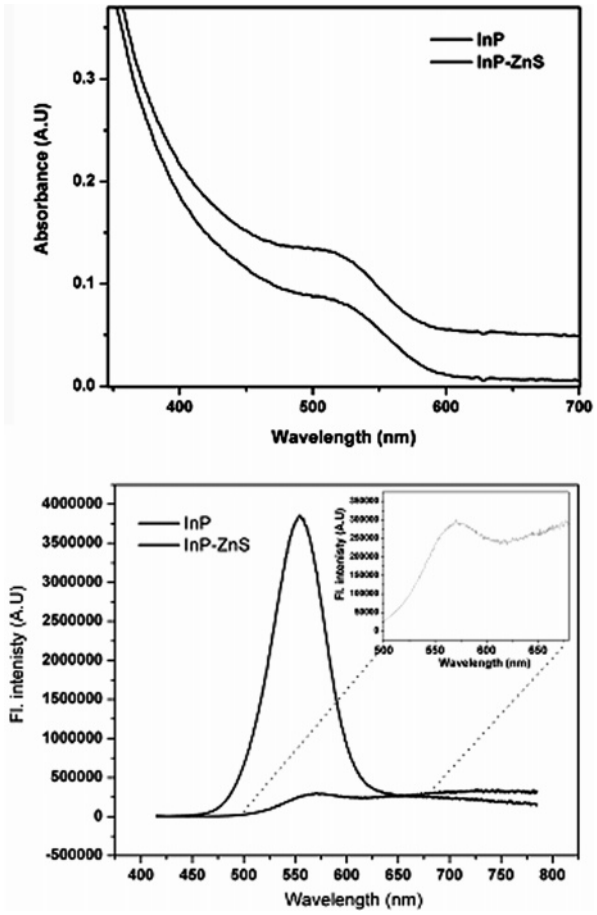

Figure 6. Absorption and emission spectra of $InP_{(QD)}$ and $InP-ZnS_{(QDs)}$ dispersed in chloroform. The inset in emission spectra shows the surface-state emission from bare InP particles, which is absent in case of ZnS coated core−shell particles.

capping group. With this taken into consideration, the size range reported would suggest that the size of the capping group is adding around 1.4−3.1 nm to the size of the particles. When these samples were prepared, free octylamine was added to fully disperse the QDs; the free amine would most likely cluster around the individual QDs, which may change the effective diameter significantly. Similar anamoly in size measurements between DLS and TEM has been observed in the literature.[14]

Optical Properties of InP−ZnS QDs. Figure 6 contains the absorption and emission spectra of $InP_{(QD)}$ and $InP-ZnS_{(QD)}$ suspensions in $CHCl_3$. The naked $InP_{(QD)}$ demonstrates an absorption feature at 510 nm, with full-width half maxima (fwhm) of 95 nm. On the basis of the UV−vis spectrum, the size of these QDs is between 20 and 26 Å.[46−48] This is in excellent agreement with the physical characterization reported above. The band edge emission of this naked $InP_{(QD)}$ sample is 571 nm, with a fwhm of 71 nm. There is also a significant amount of surface-state luminescence apparent in the PL emission spectra of the naked $InP_{(QD)}$, centered at about 726 nm.[21,38] After passivating the surface with a wider band gap semiconductor, ZnS, the surface-state emission is dramatically decreased and the quantum efficiency of the band edge

(46) Fu, H. X.; Zunger, A. *Phys. Rev. B* **1997**, *56*, 1496−1508.
(47) Micic, O. I.; Sprague, J.; Lu, Z.; Nozik, A. J. *Appl. Phys. Lett.* **1996**, *68*, 3150−3152.
(48) Micic, O. I.; Curtis, C. J.; Jones, K. M.; Sprague, J. R.; Nozik, A. J. *J. Phys. Chem.* **1994**, *98*, 4966−4969.

luminescence is improved.[18,38,46,49−57] The absorption feature is at about 507 nm with a fwhm of 90 nm, while the PL emission feature is centered at 555 nm, with a fwhm of 62 nm. It is apparent that the band-edge luminescence has blue-shifted by 16 nm. Generally, as the size of the QDs increases, their emission red-shifts; however, in this particular circumstance, though the size of the core/shell particle is increasing, the size of the core QD, which is the luminescent species, stays the same. The slight blue-shift is most likely a result of removing a second resonance (the surface state emission), and thus in the $InP-ZnS_{(QD)}$, only the actual band-edge emission is observed.

PL quantum yield of the $InP_{(QD)}$ as well as $InP-ZnS_{(QDs)}$ were measured by comparing their emission with absorption (optical density) matched solution of Coumarin 540A (Exciton Inc., quantum yield = 0.4). The PL quantum yield of the $InP_{(QD)}$ initially was less than 0.5%, but after shell growth, it dramatically increased to 15%. This value is comparable to that reported in the literature for $InP_{(QD)}$. Since there have been a few reports of high two-photon excitation cross section of CdSe and CdSe−ZnS QDs,[58,59] we also attempted to obtain two-photon excited emission spectra (Figure 7a) as well as the two-photon excitation spectra (Figure 7b) of the $InP-ZnS_{(QDs)}$.

The measured two-photon excitation cross sections are the product of the nonlinear two-photon absorption cross section σ_{2P} and the fluorescence quantum efficiency (Φ) and provide a direct measure of brightness for two-photon imaging.[60] The two-photon emission spectrum was centered around 553 nm, with a fwhm of 40 nm. This apparent narrowing of emission spectra can be due to size-selective two-photon excitation. The two-photon efficiency for these nanoparticles was sufficient enough to use them for two-photon imaging.

Folic Acid Targeted Delivery of QDs. Confocal images of the internalized QD−FA inside the cells were obtained after different time intervals of incubation. The confocal fluorescence images of KB cells treated with QD−FA at the time interval of 1, 2, 3, 6, and 18 h together with the localized PL emission spectra are shown in the Figure 8.

Over the course of the first 3 h, the uptake of the QD−FA is gradually increasing as observed by a gradual increase of fluorescence intensity within the cells, and the QDs seem to be distributed throughout the cytoplasm. After the 3 h sample, the KB cells seem to continue internalization of QD−FA, with increased accumulation in specific organelles within the cells. The localized spectrum confirms that the observed fluorescence

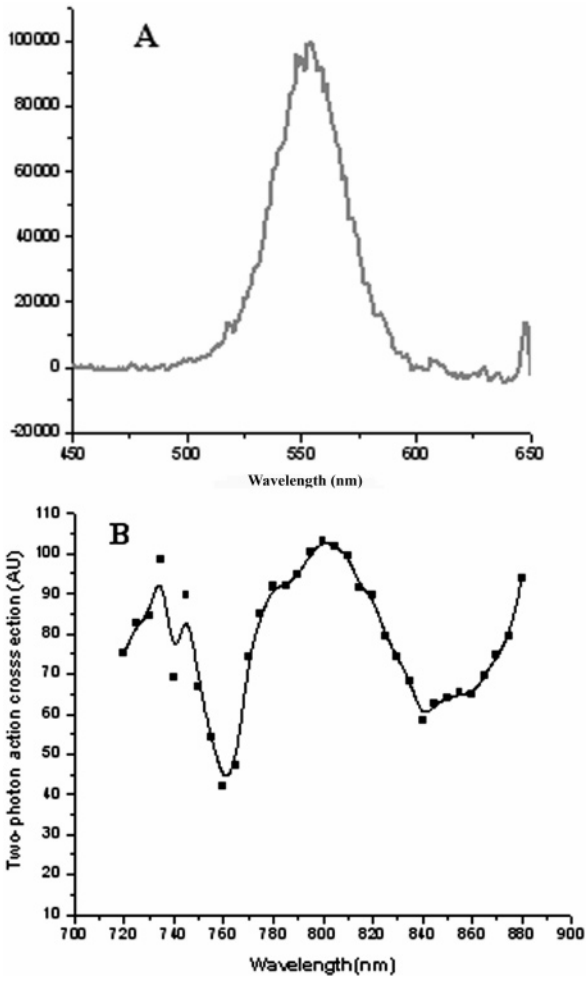

Figure 7. (a) Two-photon emission spectra. (b) Two-photon excitation spectra of $InP-ZnS_{(QDs)}$.

is from internalized QD rather than from any type of autofluorescence (Figure 8).

The accumulation of islands of QDs after 3 h are due to the onset of the formation vesicular bodies near the nucleus known as multivesicular bodies (MVBs), (basically an intermediate stage of endosome formation). There are a few reports of folate-mediated endocytosis of drugs and dyes accumulating in MVBs.[61−64] In the case of our experiments, the formation of MVBs seems to be evident, especially any time after 6 h of incubation. After overnight incubation, most of the QDs are still found in the MVBs but at a higher concentration. The accumulation in MVBs, with minimal distribution in other cytosolic organelles, strongly supports receptor-mediated endocytosis of QD−FA.

To support the receptor-mediated endocytosis of QD−FA, cells which are known to lack folic acid receptors (A549) were treated with QD−FA and imaged under similar conditions. We also conducted competition experiments, where cells were first saturated with excess free FA and subsequently incubated with

(49) Micic, O. I.; Nozik, A. J. *J. Lumin.* **1996**, *70*, 95−107.
(50) Micic, O. I.; Sprague, J.; Lu, Z. H.; Nozik, A. J. *Appl. Phys. Lett.* **1996**, *68*, 3150−3152.
(51) Bertram, D.; Micic, O. I.; Nozik, A. J. *Phys. Rev. B: Condens. Matter* **1998**, *57*, R4265−R4268.
(52) Langof, L.; Ehrenfreund, E.; Lifshitz, E.; Micic, O. I.; Nozik, A. J. *J. Phys. Chem. B* **2002**, *106*, 1606−1612.
(53) Micic, O. I.; Cheong, H. M.; Fu, H.; Zunger, A.; Sprague, J. R.; Mascarenhas, A.; Nozik, A. J. *J. Phys. Chem. B* **1997**, *101*, 4904−4912.
(54) Micic, O. I.; Jones, K. M.; Cahill, A. G.; Sprague, J. R.; Zaban, A.; Lu, Z. H.; Nozik, A. J. *Abstr. Pap. Am. Chem. Soc.* **1997**, *213*, 318-PHYS.
(55) Micic, O. I.; Nozik, A. J.; Lifshitz, E.; Rajh, T.; Poluektov, O. G.; Thurnauer, M. C. *J. Phys. Chem. B* **2002**, *106*, 4390−4395.
(56) Langof, L.; Fradkin, L.; Ehrenfreund, E.; Lifshitz, E.; Micic, O. I.; Nozik, A. J. *Chem. Phys.* **2004**, *297*, 93−98.
(57) Haubold, S.; Haase, M.; Kornowski, A.; Weller, H. *Chemphyschem* **2001**, *2*, 331−334.
(58) Larson, D. R.; Zipfel, W.; Clark, S.; Bruchez, M.; Wise, F.; Webb, W. W. *Biophys. J.* **2003**, *84*, 23a-23a.
(59) Larson, D. R.; Zipfel, W. R.; Williams, R. M.; Clark, S. W.; Bruchez, M. P.; Wise, F. W.; Webb, W. W. *Science* **2003**, *300*, 1434−1436.
(60) Xu, C.; Zipfel, W.; Shear, J. B.; Williams, R. M.; Webb, W. W. *Proc. Natl. Acad. Sci. USA* **1996**, *93*, 10763−10768.
(61) Turek, J. J.; Leamon, C. P.; Low, P. S. *J. Cell Sci.* **1993**, *106*, 423−430.
(62) Quintana, A.; Raczka, E.; Piehler, L.; Lee, I.; Myc, A.; Majoros, I.; Patri, A. K.; Thomas, T.; Mule, J.; Baker, J. R. *Pharmaceut. Res.* **2002**, *19*, 1310−1316.
(63) Holladay, S. R.; Yang, Z. F.; Kennedy, M. D.; Leamon, C. P.; Lee, R. J.; Jayamani, M.; Mason, T.; Low, P. S. *Biochim. Biophys. Acta* **1999**, *1426*, 195−204.
(64) Lu, J. Y.; Lowe, D. A.; Kennedy, M. D.; Low, P. S. *J. Drug Targeting* **1999**, *7*, 43−53.

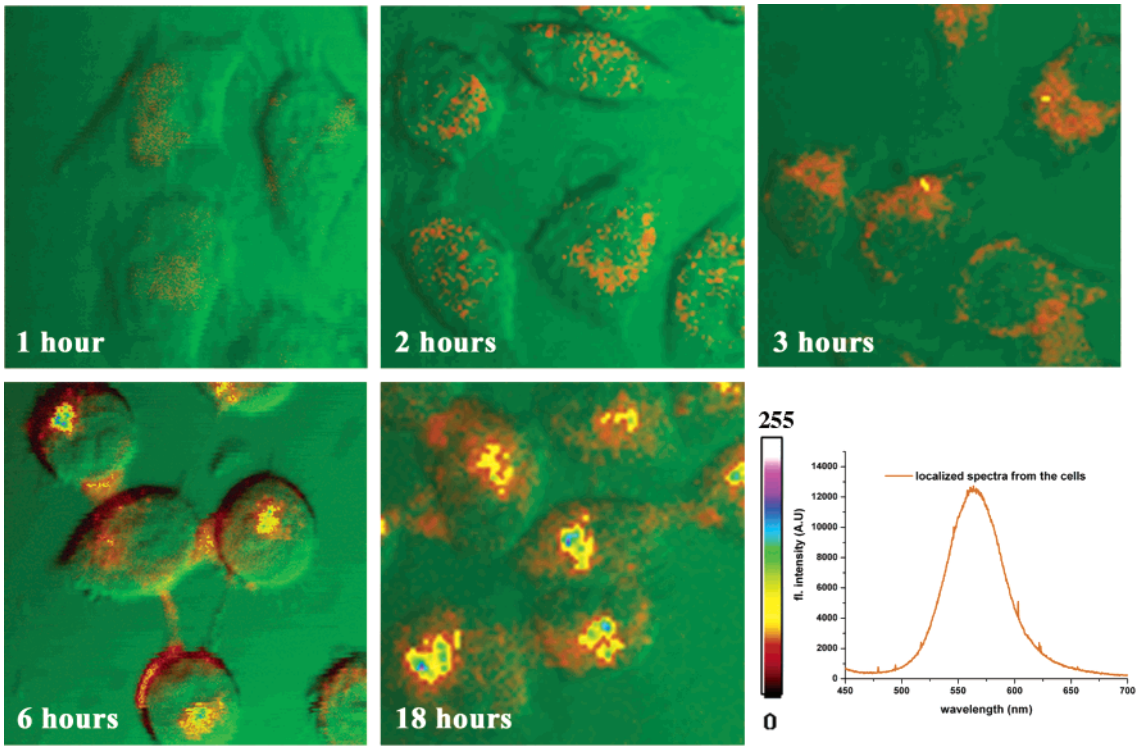

Figure 8. Confocal images showing fluorescence of QD−FA in KB cells and a localized PL emission spectrum. Here green channel shows the transmission images, while the intensity-coded (red to white) channel shows the fluorescence.

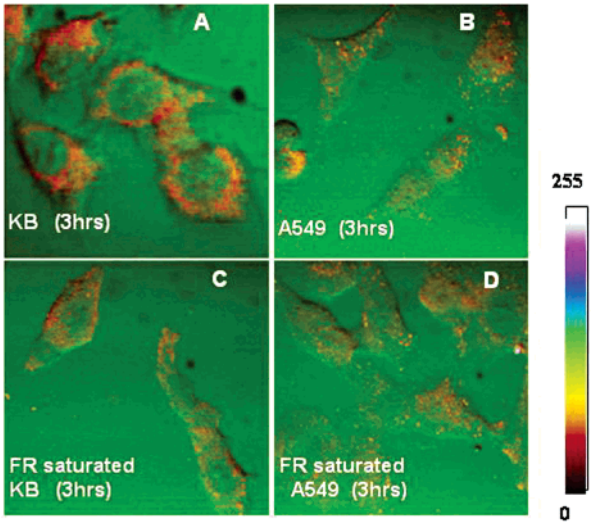

Figure 9. Confocal images showing fluorescence of QD−FA after 3 h of incubation in (A) KB cells, (B) A549 cells, (C) KB cells with excess folic acid treatment for FR saturation, and (D) A549 cells with excess folic acid treatment. Here green channel shows the transmission images, while the intensity-coded (red to white) channel shows the fluorescence.

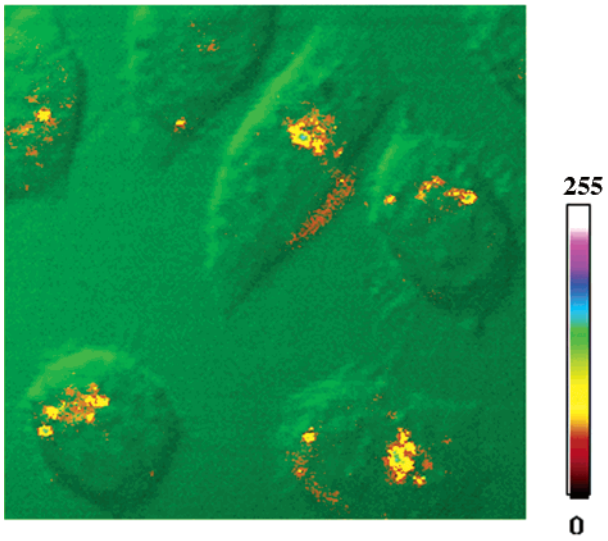

Figure 10. Two-photon image of KB cells treated with QD−FA for 6 h.

QD−FA. The obtained confocal images after 3 h of incubation are shown in Figure 9.

After 1 and 2 h of incubation with QD−FA, for folic acid saturated KB cells and A549 cells with or without FR saturation, no detectable internalization was observed (result not shown). However after 3 h, small amounts of internalized QD−FA were observed in the cells (parts B−D of Figure 9). The reduced uptake of QD−FA by receptor-negative A549 cells as well as FR-saturated KB cells is clearly seen in Figure 9B and Figure 9C, when compared with KB cells under similar conditions (Figure 9A). At the same time, folic acid saturation of A549 cells had no significant effect in their QD−FA uptake (compare parts B and D of Figure 9).

In A549 cells, longer incubation periods showed a slight increase in the cytoplasmic staining, though not as strong as in the KB cells with similar incubation periods (results in Supporting Information). This uptake, through an unknown endocytic pathway, is significantly different from the receptor-mediated entry in the KB cells.

Similar results were observed for MCF-7 cells which are also known to be FR negative (results in Supporting Information). This confirms the mode of internalization in cells containing FR is indeed receptor mediated.

Two-Photon Imaging with QDs. Since we observed significant two-photon fluorescence from InP−$ZnS_{(QDs)}$, we at-

tempted direct two-photon imaging with QD−FA. Figure 10 shows the two-photon images of KB cells treated with QD−FA for 6 h.

The cells imaged in Figure 10 were prepared exactly as described in the case of the KB cells imaged after 6 h in Figure 8. This figure demonstrates that upon accumulation of QDs into MVBs in FR-rich cells (KB cells for this particular study), they can be imaged directly by two-photon techniques. This potential for multiphoton imaging provides the possibility for longer term imaging of cellular processes, with less photodamage than UV-excited imaging. QDs are a key probe for multicolor fluorescence microscopy and may prove to be especially useful for multiphoton microscopy, where bright and photostable probes are needed for various complex imaging tasks at hand.

Conclusion

We have prepared photostable water-dispersible $InP-ZnS_{(QDs)}$ by a new fast reaction. These MAA-coated nanoparticles are readily conjugated with folic acid for targeted bioimaging. By use of confocal microscopy, two-photon microscopy, and localized spectroscopy, we have demonstrated the internalization of QD−FA in FR overexpressing tumor cells such as human oral epidermoid carcinoma cells (KB). The receptor-mediated uptake of QD−FA in KB cells is confirmed by the rapid uptake (in less than 1 h) and the formation of MVBs (incubation periods over 6 h). The inhibition of internalization of QD−FA by free folic acid in KB cells and the reduced uptake of QD−FA by known FR-negative cell lines (A549) confirmed this receptor-mediated process.

Bioimaging is an important area of research with QDs. All current studies in the literature are based on II−VI QDs (specifically CdSe) as the luminescence probe. These QDs are ionic solids, which in the presence of water will readily ionize. The ionization of CdSe will form Cd^{2+} and Se^{2-} in aqueous environments. These ions are very toxic in trace quantities in the human body. For these reasons, we have prepared potentially less toxic InP-based QDs and conducted cellular imaging. Future work within our group will focus on increasing the quantum yield of the InP−ZnS nanoparticles and varying the surface functionalization of the nanoparticles to effectively eliminate adsorbed water at the nanoparticle surface. Work on using other targeting moieties for QDs, detailed cell viability studies, and cytotoxicity comparison of II−VI and III−V compounds are also in progress.

Acknowledgment. This work was supported in part by a DURINT grant from the Directorate of chemistry and life sciences of the Air Force office of scientific research and in part be a grant from the OISHEI foundation. Partial support from the Center of Excellence in Bioinformatics and Life Sciences of the University of Buffalo is also acknowledged. We thank Dr. Graheme Williams and Ms, Julia Salas of Brookhaven Instruments for helping us with the particle size measurements using DLS. The authors also thank Ms. Lisa Vathy for help with cell culture and Dr. James E. Bergey for useful discussions.

Supporting Information Available: TEM images of InP and InP/ZnS nanoparticles (Figure S1), methods describing QD−FA uptake in receptor negative MCF-7 cells and A-549 cells, confocal images showing fluorescence of QD−FA in MCF-7 cells (receptor-negative cell line) after 1, 3, and 6 h of incubation (Figure S2), and confocal images showing fluorescence of QD−FA in A-549 cells (receptor-negative cell line) after 1, 3, and 6 h of incubation (Figure S3). This material is available free of charge via the Internet at http:// pubs.acs.org.

JA051455X